WEAK INTERACTION, NUCLEAR PHYSICS AND SUPERNOVAE*

K. Langanke

GSI and Technische Universität Darmstadt, Germany

(Received January 7, 2008)

Nuclear physics plays an essential role in the dynamics of a type II supernova (a collapsing star). Recent advances in nuclear many-body theory allow now improved calculations of the stellar weak-interaction rates involving nuclei. The most important process is the electron capture on finite nuclei with mass numbers $A > 55$. This process is the source of neutrinos during the collapse phase. Neutrino–nucleus reactions occur during the collapse and explosion phase. They play an interesting role for supernova nucleosynthesis. Spectroscopy by supernova neutrino detectors is a fascinating goal for the observation of the next close-by supernova.

PACS numbers: 97.60.Bw, 26.30.+k, 26.50.+x

1. Introduction

Besides his many other scientific interests, Ziemek Sujkowski was strongly fascinated by weak-interaction physics as probe for detailed nuclear structure and as a potential tool to glimpse beyond the standard model of particle physics. A third important motivation certainly has been astrophysics where weak interaction processes play crucial roles for the evolution and dynamics of many astrophysical objects. Perhaps core-collapse supernovae are the most important examples. The aim of this manuscript is to summarize recent developments in the description of weak-interaction processes with relevance for core-collapse supernovae.

Massive stars end their lives as type II supernovae, triggered by a collapse of their central iron core with a mass of more than $1M_{\odot}$. The general picture of a core-collapse supernova is probably well understood and has been confirmed by various observations from supernova 1987A. It can be briefly summarized as follows: At the end of its hydrostatic burning stages, a massive star has an onion-like structure with various shells where nuclear burning still proceeds (hydrogen, helium, carbon, neon, oxygen and silicon

* Presented at the XXX Mazurian Lakes Conference on Physics, Piaski, Poland, September 2–9, 2007.

shell burning). As nuclei in the iron/nickel range have the highest binding energy per nucleon, the iron core in the star's center has no nuclear energy source to support itself against gravitational collapse. As mass is added to the core, its density and temperature raises, finally enabling the core to reduce its free energy by electron captures of the protons in the nuclei. This reduces the electron degeneracy pressure and the core temperature, as the neutrinos produced by the capture can initially leave the star unhindered. Both effects accelerate the collapse of the star. With increasing density, neutrino interactions with matter become decisively important and neutrinos have to be treated by Boltzmann transport. Nevertheless, the collapse proceeds until the core composition is transformed into neutron-rich nuclear matter. Its finite compressibility brings the collapse to a halt, a shock wave is created which traverses outwards through the infalling matter of the core's envelope. This matter is strongly heated and dissociated into free nucleons. Due to current models the shock has not sufficient energy to explode the star directly. It stalls, but is shortly after revived by energy transfer from the neutrinos which are produced by the cooling of the neutron star born in the center of the core. The neutrinos carry away most of the energy generated by the gravitational collapse and a fraction of the neutrinos are absorbed by the free nucleons behind the stalled shock. The revived shock can then explode the star and the stellar matter outside of a certain mass cut is ejected into the Interstellar Medium. A brief sketch of the various supernova phases is given in Fig. 1. Due to the high temperatures associated with the shock's passage, nuclear reactions can proceed rather fast giving rise to explosive nucleosynthesis which is particularly important in the deepest layers of the ejected matter. Reviews on core-collapse supernovae can be found in [1, 2].

The most sophisticated spherical supernova simulations, including detailed neutrino transport [3–5], failed to explode indicating that improved input or numerical treatment was required. Recently it turned out that the picture changes if multi-dimensional hydrodynamical effects like convection or plasma instabilities are appropriately taken into account. So different groups find successful explosions in full two-dimensional simulations [6, 7]. Among the microscopic inputs which have been decisively improved in recent years were nuclear processes mediated by the weak interaction, where progress has been made possible by improved many-body models and better computational facilities, as is summarized in [8]. Here we focus on the electron capture on nuclei, which strongly influences the dynamics of the collapse and produces the neutrinos present during the collapse, on neutrino–nucleus reactions and their impact on the neutrino opacity, and finally on recent developments in explosive nucleosynthesis, where again neutrino-induced reactions are essential.

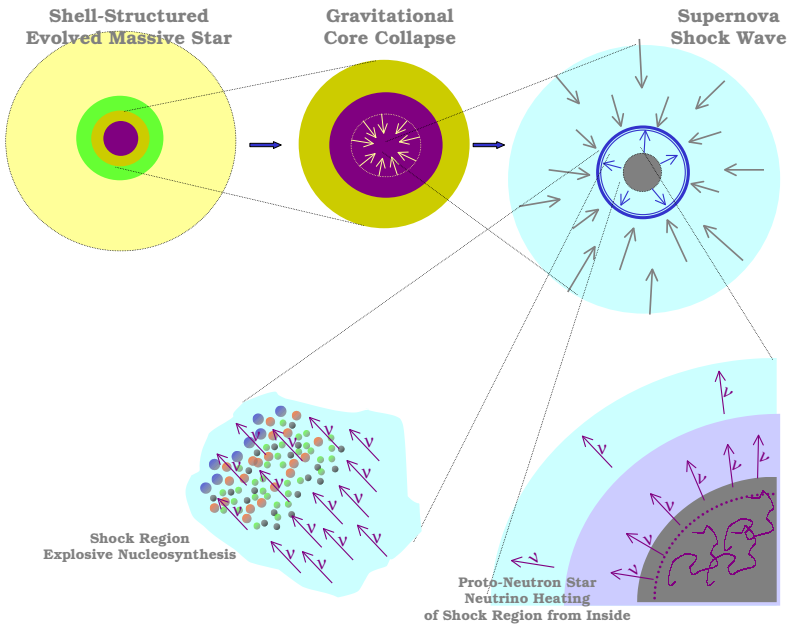

Fig. 1. Schematic stages of the collapse of a massive star and a supernova explosion (courtesy of Roland Diehl).

2. Electron captures in core-collapse supernovae

During the collapse electrons can be described by a degenerate relativistic gas. The Fermi energy $E_{\rm F}$ of the electrons scales with the density ρ as $E_{\rm F} \sim \rho^{1/3}$ and reaches values of order 10 MeV at a few 10^{10} g/cm^3. This rather large value effectively unables β-decays (which, however, play some role during silicon burning [9,10]), but favors electron captures. As electron captures reduce the electron-to-nucleon ratio Y_e and change protons into neutrons, the nuclei abundant in the core become more neutron-rich and heavier, as nuclei with decreasing Z/A ratios are more bound in heavier nuclei.

For densities $\rho < 10^{11}$ g/cm^3, electron captures are dominated by Gamow–Teller (GT) transitions. At higher densities forbidden transitions have to be included as well. In the early stage of the collapse ($\rho < 10^{10}$ g/cm^3) the core composition is dominated by nuclei from the iron mass range (pf-shell nuclei with mass numbers $A \approx 45$–65). During this collapse phase, one has $E_{\rm F} \sim Q$ (Q is the mass difference of parent and daughter nuclei), and hence a reliable derivation of the capture rate requires an accurate detailed description of the GT strength distributions for the thermal ensemble of parent states. It has been demonstrated in [11,12] that modern shell model

calculations are capable to describe nuclear properties relevant to derive stellar electron capture rates (spectra and GT_+ distributions) rather well (an example is shown in Fig. 2) and are therefore the appropriate tool to calculate the weak-interaction rates for nuclei with $A \sim 50$–65. Impressive progress has been recently achieved by experimentally determining GT_+ distributions by $(d, {}^2\mathrm{He})$ charge-exchange reactions with an energy resolution of about 150 keV [13–16] (see Fig. 2).

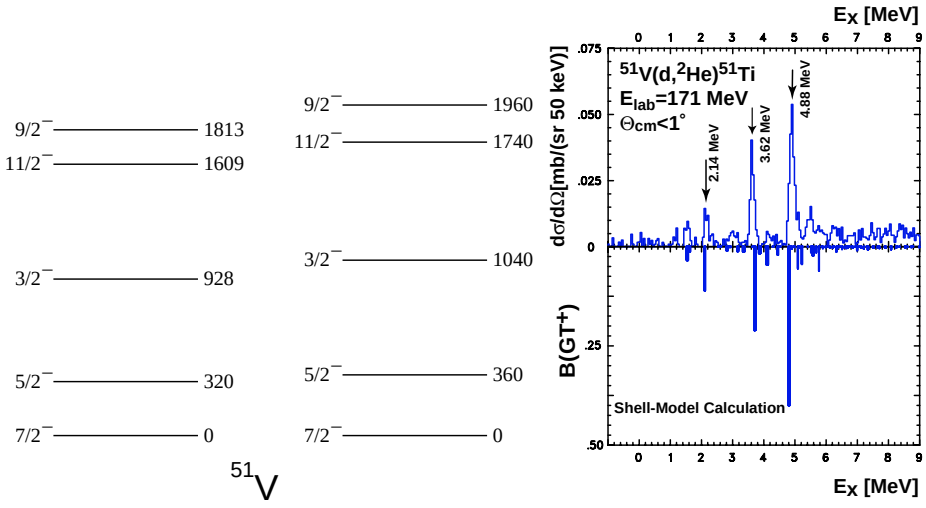

Fig. 2. Comparison of the measured spectrum (left) and $^{51}\mathrm{V}(d,{}^2\mathrm{He})^{51}\mathrm{Ti}$ cross section (right) at forward angles (which is proportional to the GT_+ strength) with the shell model spectrum and GT distribution in $^{51}\mathrm{V}$ (partially from [13]).

With increasing densities, E_F becomes sufficiently larger than the respective nuclear Q values and the capture rate becomes less sensitive to the detailed GT_+ distribution and is mainly dependent only on the total GT strength. Thus, less sophisticated nuclear models might be sufficient. However, one is facing a nuclear structure problem which has been overcome only recently. Once the matter has become sufficiently neutron-rich, nuclei with proton numbers $Z < 40$ and neutron numbers $N > 40$ will be quite abundant in the core. For such nuclei, Gamow–Teller transitions would be Pauli forbidden (GT_+ transitions change a proton into a neutron in the same harmonic oscillator shell), were it not for nuclear correlation and finite temperature effects which move nucleons from the pf shell into the gds shell (Fig. 3). To describe such effects in an appropriately large model space (*e.g.* the complete $fpgds$ shell) is currently only possible by means of the Shell Model Monte Carlo approach (SMMC) [17, 18]. In [19] SMMC-based electron capture rates have been calculated for many nuclei

which are present during the collapse phase. While the SMMC is capable of dealing with sufficiently large model spaces, the residual interaction and the single particle energies appropriate for the very neutron-rich nuclei in these large model spaces are not well determined. Here decisive progress is expected from future radioactive ion beam facilities like FAIR.

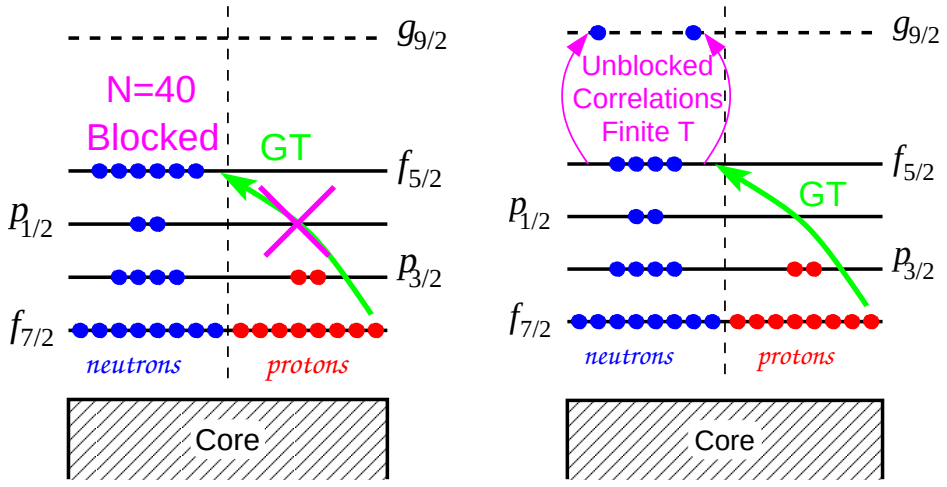

Fig. 3. In the independent particle model GT transitions are blocked at neutron number $N = 40$.

The effect of the shell model electron capture rates on the collapse has been investigated in several supernova simulations. At first, it has been observed that it has a significant impact on presupernova models which have larger iron cores and Y_e values, while the entropy, and hence the fraction of free protons, is reduced [9, 10]. In contrast to previous belief, electron capture occurs dominantly on nuclei rather than on free protons during the collapse [19] (see Fig. 4). As a consequence the core cools more efficiently by neutrino emission. However, the neutrino spectrum is shifted to smaller energies, related to the larger Q-values of neutron-rich nuclei compared to protons. Due to more efficient capturing of electrons and hence smaller Y_e (Fig. 5), the homologous core is shrunk by roughly 0.1 $M_\odot$ [19, 20] (see Fig. 6). As a consequence the shock wave has to traverse a larger amount of matter in the collapsing iron core, which also has a different temperature-density profile. However, also with the improved weak-interaction rates, the shock wave energetics and the energy transfer by neutrinos does not suffice to explode the star in spherical simulations [20, 21].

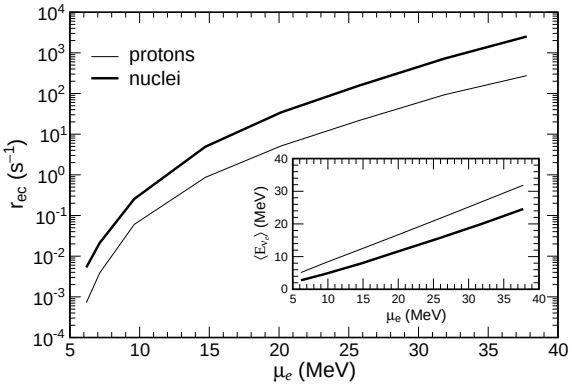

Fig. 4. The reaction rates for electron capture on protons (thin line) and nuclei (thick line) are compared as a function of electron chemical potential along a stellar collapse trajectory. The insert shows the related average energy of the neutrinos emitted by capture on nuclei and protons. The results for nuclei are averaged over the full nuclear composition (from [19]).

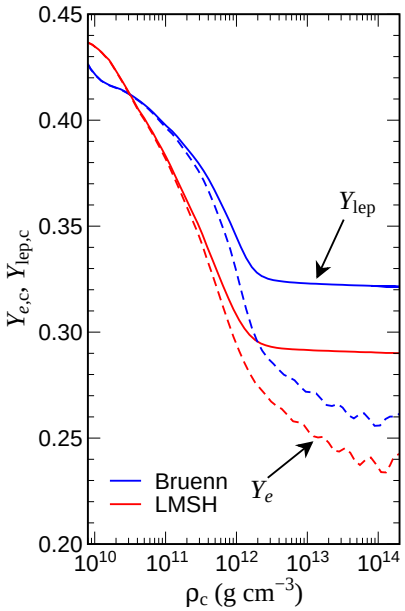

Fig. 5. The electron and lepton fraction in the center during the collapse phase. The thin line is a simulation using the Bruenn parameterization [22] (which neglects electron capture on nuclei with $N > 40$), while the thick line is for a simulation using the shell model rates (courtesy of Hans-Thomas Janka).

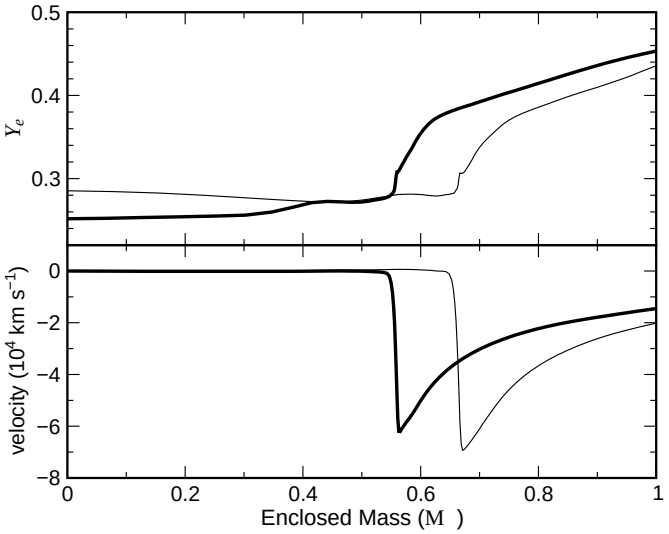

Fig. 6. The electron fraction and velocity as functions of the enclosed mass at bounce for a 15 $M_\odot$ model [9]. The thin line is a simulation using the Bruenn parameterization [22], while the thick line is for a simulation using the shell model rates (from [20]).

3. Inelastic neutrino–nucleus scattering

Elastic neutrino–nucleus and inelastic neutrino–electron scattering has been included in supernova simulations and was observed as essential for neutrino trapping and thermalization during the collapse [1]. Combining the shell model for GT transitions with an RPA approach for forbidden transitions one has recently been able to derive inelastic neutrino–nucleus cross sections for the density-temperature conditions in a supernova [23]. Importantly the theoretical approach could be validated by a detailed comparison to high-accuracy M1 data derived in electron scattering which are dominated by the same GT transition operator as required in neutrino–nucleus scattering [24].

Although inelastic neutrino–nucleus scattering contributes to the thermalization of neutrinos with the core matter, the inclusion of this process has no significant effect on the collapse trajectories. However, it has a significant effect on the spectrum of neutrinos generated in the ν_e burst just after bounce. This burst has two reasons. At first, the trapped neutrinos are released due to decreasing densities of the expanding matter. Secondly, the shock has dissociated the matter into free neutrons and protons which dramatically increases the capture of the remaining electrons as they now have to overcome much reduced Q-values. When the ν_e burst neutrinos try to

leave the star, they have to pass through relatively dense matter composed of medium-mass nuclei. By inelastic scattering, the neutrinos can excite the nuclei, and are themselves down-scattered in energy. In this way the high-energy tail of the emitted ν_e burst neutrino spectrum is significantly reduced (see Fig. 7, [25]). This makes the detection of these supernova neutrinos by earthbound detectors more difficult, as the neutrino detection cross section scales with E_ν^2. Table I summarizes the detection cross sections for several detectors and shows the reduction factors due to the consideration of inelastic neutrino–nucleus scattering.

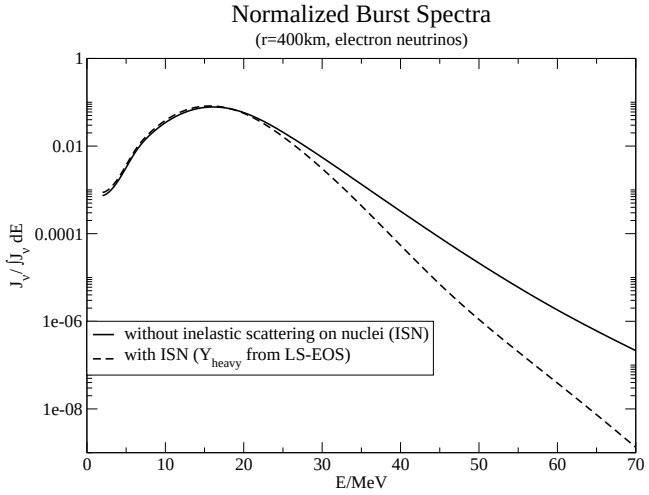

Fig. 7. Comparison of the normalized neutrino spectra, arising from the ν_e burst shortly after bounce, without (solid) and with (dashed) consideration of inelastic neutrino–nucleus scattering in the supernova simulations (from [25]).

TABLE I

Detector	Material	$\langle\sigma\rangle$ (10^{-42} cm^2) with $A(\nu,\nu')A^\star$	$\langle\sigma\rangle$ (10^{-42} cm^2) without $A(\nu,\nu')A^\star$	Change
SNO	d	4.92	5.36	8%
MiniBoone	^{12}C	0.050	0.080	37%
	^{12}C (Ngs)	0.046	0.071	35%
S-Kamiokande	^{16}O	0.0053	0.0128	58%
Icarus	^{40}Ar	13.4	15.1	11%
Minos, UNO	^{56}Fe	6.2	7.5	17%
OMNIS	^{208}Pb	103.3	124.5	17%

4. Explosive nucleosynthesis

When in an successful explosion the shock passes through the outer shells, its high temperature induces an explosive nuclear burning on short time-scales. This explosive nucleosynthesis can alter the elemental abundance distributions in the inner (silicon, oxygen) shells. More interestingly the shock has sufficiently high temperatures that nuclear binding cannot withstand and matter is ejected as free protons and neutrons from the neutron star surface. As the outflow is adiabatic, the ejected matter reaches cooler regions at larger distances and nuclei can be assembled from free nucleons. The abundance outcome obviously depends strongly on the ratio of neutrons and protons which is set by the competition of neutrino and anti-neutrino absorption on free nucleons.

Recently explosive nucleosynthesis has been investigated consistently within supernova simulations, where a successful explosion has been enforced by slightly enlargening the neutrino absorption cross section on nucleons or the neutrino mean-free path, which both increase the efficiency of the energy transport to the stalled shock. The results presented in [26, 27] showed that in an early phase after the bounce the ejected matter is actually proton-rich as the ν_e neutrinos have sufficiently large energies to drive the matter proton-rich. In later stages, *i.e.* a few seconds after bounce, the neutrino opacities in the neutron-rich matter ensure that $\bar{\nu_e}$ have larger average energies than ν_e and $\bar{\nu_e}$ absorption on protons dominates driving the matter neutron-rich (allowing for the r-process to occur).

4.1. The νp process

The studies presented in [26–28] show that matter with Y_e larger than 0.5 will always be present in core-collapse supernovae explosions with ejected matter irradiated by a strong neutrino flux, independently of the details of the explosion. As this proton-rich matter expands and cools, nuclei can form resulting in a composition dominated by $N = Z$ nuclei, mainly ^{56}Ni and ^{4}He, and protons. Without the further inclusion of neutrino and antineutrino reactions the composition of this matter will finally consist of protons, alpha-particles, and heavy (Fe-group) nuclei (in nucleosynthesis terms a proton- and alpha-rich freeze-out), with enhanced abundances of ^{45}Sc, ^{49}Ti, and ^{64}Zn [26, 27]. In these calculations the matter flow stops at ^{64}Ge with a small proton capture probability and a beta-decay half-life (64 s) that is much longer than the expansion time scale ($\sim$ 10 s) [26].

As noted by Martinez-Pinedo and explored in [29] the synthesis of nuclei with $A > 64$ can be obtained, if one explores the previously neglected effect of neutrino interactions on the nucleosynthesis of heavy nuclei. $N \sim Z$ nuclei are practically inert to neutrino capture (converting a neutron into

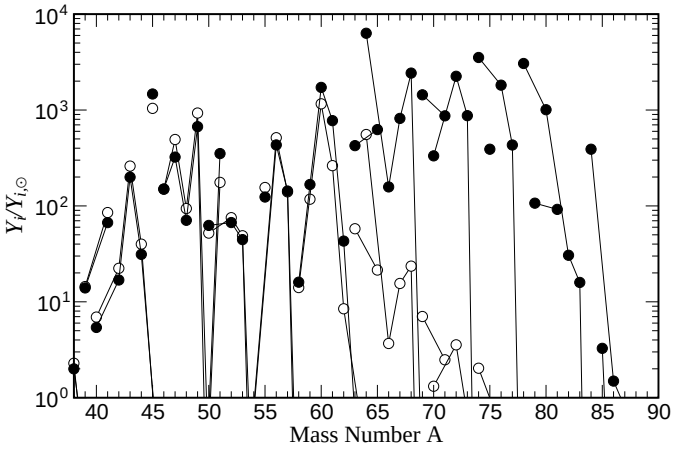

Fig. 8. Elemental abundance yields (normalized to solar) for elements produced in the proton-rich environment shortly after the supernova shock formation. The matter flow stops at nuclei like ^{56}Ni and ^{64}Ge (open circles), but can proceed to heavier elements if neutrino reactions are included during the network (full circles) (from [29]).

a proton), because such reactions are endoergic for neutron-deficient nuclei located away from the valley of stability. The situation is different for antineutrinos that are captured in a typical time of a few seconds, both on protons and nuclei, at the distances at which nuclei form ($\sim$ 1000 km). This time scale is much shorter than the beta-decay half-life of the most abundant heavy nuclei reached without neutrino interactions (*e.g.* ^{56}Ni, ^{64}Ge). As protons are more abundant than heavy nuclei, antineutrino capture occurs predominantly on protons, causing a residual density of free neutrons of 10^{14}–10^{15} cm^{-3} for several seconds, when the temperatures are in the range 1–3 GK. The neutrons produced via antineutrino absorption on protons can easily be captured by neutron-deficient $N \sim Z$ nuclei (for example ^{64}Ge), which have large neutron capture cross sections. The amount of nuclei with $A > 64$ produced is then directly proportional to the number of antineutrinos captured. While proton capture, (p, γ), on ^{64}Ge takes too long, the (n, p) reaction dominates (with a lifetime of 0.25 s at a temperature of 2 GK), permitting the matter flow to continue to nuclei heavier than ^{64}Ge via subsequent proton captures.

Fröhlich *et al.* argue that all core-collapse supernovae will eject hot, explosively processed matter subject to neutrino irradiation and that this novel nucleosynthesis process (called νp process) will operate in the innermost ejected layers producing neutron-deficient nuclei above $A > 64$. However, how far the mass flow within the νp process can proceed, strongly

depends on the environment conditions, most notably on the Y_e value of the matter. Obviously the larger Y_e, the larger the abundance of free protons which can be transformed into neutrons by antineutrino absorption. Fig. 9 shows the dependence of the νp process abundances as a function of the Y_e value of the ejected matter. Nuclei heavier than $A = 64$ are only produced for $Y_e > 0.5$, showing a very strong dependence on Y_e in the range 0.5–0.6. A clear increase in the production of the light p-nuclei, ^{92,94}Mo and ^{96,98}Ru, is observed as Y_e gets larger. Thus the νp process offers the explanation for the production of these light p-nuclei, which was yet unknown. It might also explain the presence of strontium in the extremely metalpoor, and hence very old, star HE 1327-2326 [30]. The νp process results of Fröhlich *et al.* have been recently confirmed by Pruet *et al.* [31], in a study of the nucleosynthesis that occurs in the early proton-rich neutrino wind.

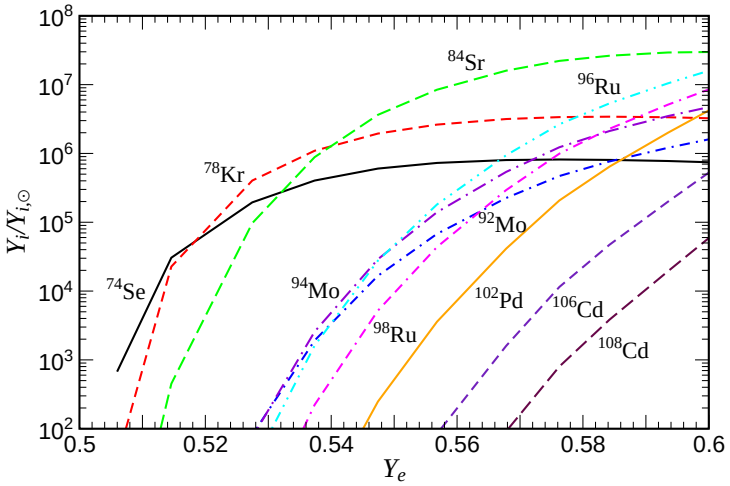

Fig. 9. Light p-nuclei abundances in comparison to solar abundances as a function of Y_e. The Y_e-values given are the ones obtained at a temperature of 3 GK that corresponds to the moment when nuclei are just formed and the νp process starts to act (from [29]).

4.2. The r-process

About half of the elements heavier than mass number $A \sim 60$ are made within the r-process, a sequence of rapid neutron captures and β-decays [32, 33]. The process is thought to occur in environments with extremely high neutron densities [34]. Then neutron captures are much faster than the competing decays and the r-process path runs through very neutron-rich, unstable nuclei. Once the neutron source ceases, the process stops and the produced nuclides decay towards stability producing the neutron-rich heavier elements.

Despite many promising attempts the actual site of the r-process has not been identified yet. However, parameter studies have given clear evidence that the observed r-process abundances cannot be reproduced at one site with constant temperature and neutron density [35]. Thus the abundances require a superposition of several (at least three) r-process components. This likely implies a dynamical r-process in an environment in which the conditions change during the duration of the process. The currently favored r-process sites (type II supernovae [36] and neutron-star mergers [37]) offer such dynamical scenarios. However, recent meteoritic clues might even point to more than one distinct site for our solar r-process abundance [38]. The same conclusion can be derived from the observation of r-process abundances in low-metalicity stars [39], a milestone of r-process research.

The r-process path runs through such extremely neutron-rich nuclei that most of their properties (*i.e.* mass, lifetime and neutron capture cross sections) are experimentally unknown and have to be modelled, based on experimental guidance. Arguably the most important nuclear ingredient in r-process simulations are the nuclear masses as they determine the flow-path. They are traditionally modelled by empirical mass formulae parametrized to the known masses [40, 41]. A new era has been opened very recently, as for the first time, nuclear mass tables have been derived on the basis of nuclear many-body theory (Hartree-Fock–Bogoliobov model) [42–44] rather than by parameter fit to data.

The nuclear half-lives strongly influence the relative r-process abundances. In a simple β-flow equilibrium picture the elemental abundance is proportional to the half-life, with some corrections for β-delayed neutron emission [45]. As r-process half-lives are longest for the magic nuclei, these waiting point nuclei determine the minimal r-process duration time; *i.e.* the time needed to build up the r-process peak around $A \sim 200$. We note, however, that this time depends also crucially on the r-process path and can be as short as a few 100 milliseconds if the r-process path runs close to the neutron dripline.

There are a few milestone half-life measurements including the $N = 50$ waiting point nuclei ^{80}Zn and ^{79}Cu and the $N = 82$ waiting point nuclei ^{130}Cd and ^{129}Ag [46, 47]. Although no half-lives for $N = 126$ waiting points have yet been determined, there has been decisive progress towards this goal recently [48].

These data play crucial roles in constraining and testing nuclear models which are still necessary to predict the bulk of half-lives required in r-process simulations. It is generally assumed that the half-lives are dominated by allowed Gamow–Teller (GT) transitions, with forbidden transitions contributing noticeably for the heavier r-process nuclei [49]. The β-decays only probe the weak low-energy tail of the GT distributions and provide

quite a challenge to nuclear modelling as they are not constrained by sum rules. Traditionally the estimate of the half-lives are based on the quasi-particle random phase approximation (QRPA) on top of the global FRDM or ETFSI models [41, 50]. Recently half-lives for selected (spherical) nuclei have been presented using the QRPA approach based on the microscopic Hartree-Fock–Bogoliubov method [51] or a global density functional [52,53]; in particular the later approach achieved quite good agreement with data for spherical nuclei in different ranges of the nuclear chart. Applications of the interacting shell model [54–56] have yet been restricted to waiting point nuclei with magic neutron numbers. Here, however, this model, which accounts for correlations beyond the QRPA approach, obtains quite good results (for an example see Fig. 10).

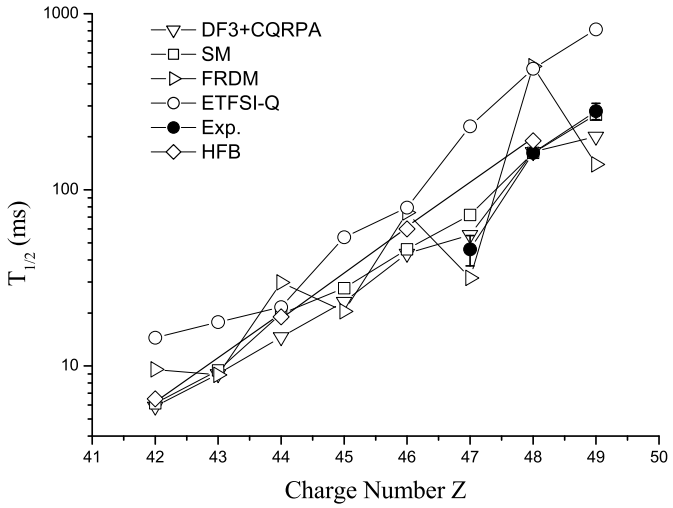

Fig. 10. Comparison of various theoretical half-life predictions with data for the $N = 82$ r-process waiting points (from [56]).

Fig. 11 shows the impact of the half-lives of the waiting point nuclei with magic neutron numbers $N = 82$ on the r-process abundances. One simulation has been performed with a standard set of half-lives [40]. In the other the half-lives for the spherical nuclei approaching the $N = 82$ shell closure have been replaced by those based on the density functional approach [53]. The latter are noticeably shorter than the standard set and agree quite well with the available data (see Fig. 10). One clearly observes that the shorter half-lives allow for a significantly larger mass flow to heavier nuclei.

If the r-process occurs in strong neutrino fluences, different neutrino-induced charged-current (*e.g.* (ν_e, e^-)) and neutral-current (*e.g.* (ν, ν')) reactions, which are often accompanied by the emission of one or several neutrons [57–59], have to be modelled and included as well. Recently neutrino-induced fission has been suggested to explain the robust r-process pattern observed in old, metalpoor stars [60]. Respective fission rates and yield distributions have been calculated on the basis of the RPA model [61, 62]. However, very recent r-process simulations which accounted for all different fission processes (spontaneous, neutron-, beta- and neutrino-induced fission) and their yield distributions [63] indicate that neutrino-induced fission is likely to be unimportant [64, 65].

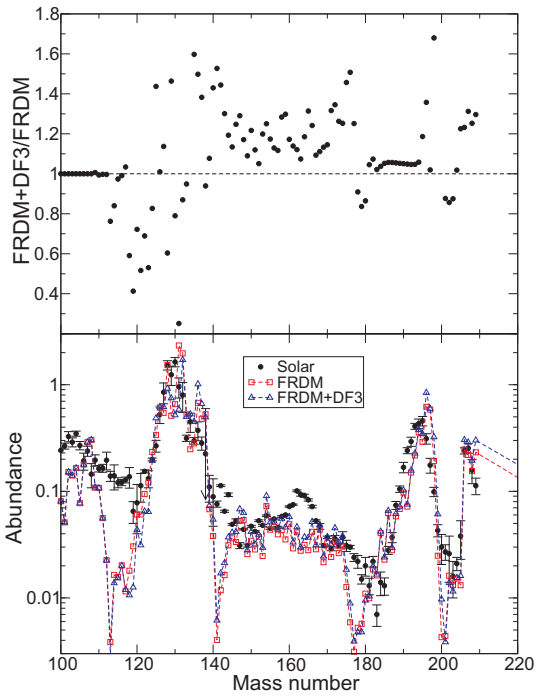

Fig. 11. Lower panel: the observed solar r-process abundance distribution compared to the r-process abundances calculated (a) with the FRDM half-lives of [40] for all nuclei in the network and (b) with the half-lives for the $Z = 42$–49 isotope chains replaced by the half-lives of [53]. Upper panel: the ratio of the r-process abundances calculated within (a) and (b) as a function of the mass number (from [53]).

5. Conclusions

The recent advances in nuclear many-body modelling has led to noticeable improvements in the nuclear input for core-collapse supernova models. It has been proven that the dynamical timescale of the final collapse is dominated by electron capture on nuclei, and not, as has been the standard picture for many years, by capture on free protons. This has significant consequences for the collapse and changes the Y_e and density profiles throughout the core. However, first supernova simulations do not yield successful explosions. In the meantime, several minor improvements with respect to the incorporation of electron capture in collapse simulations have been derived. These include a consistent treatment of plasma screening corrections which reduce the rates, but apparently lead to no significant changes in the simulations. Further, detailed neutrino spectra have been derived for the capture on individual nuclei (and their NSE average) as function of temperature, density and Y_e values. Possible consequences are expected to be small, but need to be explored.

In the hot supernova environment fast nuclear reactions occur giving rise to an explosive nucleosynthesis. On quite general grounds it has been argued recently that the matter in the deepest ejected layers will be rich in protons, set by the competition of neutrino and antineutrino absorption on free nucleons. Nucleosynthesis in such an environment with $Y_e > 0.5$ has been shown to produce proton-rich nuclei with masses $A > 64$ and might be the until now unknown astrophysical site for the production of the light p-nuclei like ^{92,94}Mo and ^{96,98}Ru.

The work presented here has benefited from fruitful discussions and collaborations with Gabriel Martinez-Pinedo, I. Borzov, David Dean, Carla Fröhlich, Alexander Heger, Raphael Hix, Thomas Janka, Andrius Juodagalvis, Aleksandra Kelic, Tony Mezzacappa, Matthias Liebendörfer, Jorge Sampaio, Karl-Heinz Schmidt, F.-K. Thielemann and Stan Woosley.

REFERENCES

[1] H.A. Bethe, *Rev. Mod. Phys.* **62**, 801 (1990).

[2] H.-Th. Janka, K. Kifonidis, M. Rampp, *Lect. Notes Phys.* **578**, 333 (2001).

[3] R. Buras, M. Rampp, H.-Th. Janka, K. Kifonidis, *Phys. Rev. Lett.* **90**, 241101 (2003).

[4] H.Th. Janka, M. Rampp, *Astrophys. J.* **539**, L33 (2000).

[5] A. Mezzacappa *et al.*, *Phys. Rev. Lett.* **86**, 1935 (2001).

[6] A. Burrows *et al.*, *Astrophys. J.* **640**, 878 (2006).

[7] A. Marek, Ph.D. Thesis, TU Munich 2006; H.-Th. Janka, A. Marek, to be published.

[8] K. Langanke, G. Martínez-Pinedo, *Rev. Mod. Phys.* **75**, 819 (2003).

[9] A. Heger, K. Langanke, G. Martínez-Pinedo, S.E. Woosley, *Phys. Rev. Lett.* **86**, 1678 (2001).

[10] A. Heger, S.E. Woosley, G. Martínez-Pinedo, K. Langanke, *Astrophys. J.* **560**, 307 (2001).

[11] E. Caurier, K. Langanke, G. Martínez-Pinedo, F. Nowacki, *Nucl. Phys.* **A653**, 439 (1999).

[12] K. Langanke, G. Martínez-Pinedo, *Nucl. Phys.* **A673**, 481 (2000).

[13] C. Bäumer *et al.*, *Phys. Rev.* **C68**, 031303(R) (2003).

[14] M. Hagemann *et al.*, *Phys. Lett.* **B579**, 251 (2004).

[15] C. Bäumer *et al.*, *Phys. Rev.* **C71**, 024603 (2005).

[16] M. Hagemann *et al.*, *Phys. Rev.* **C71**, 014606 (2005).

[17] K. Langanke *et al.*, *Phys. Rev.* **C52**, 718 (1995).

[18] S.E. Koonin, D.J. Dean, K. Langanke, *Phys. Rep.* **278**, 2 (1997).

[19] K. Langanke *et al.*, *Phys. Rev. Lett.* **90**, 241102 (2003).

[20] R.W. Hix *et al.*, *Phys. Rev. Lett.* **91**, 210102 (2003).

[21] H.-Th. Janka *et al.*, *Phys. Rep.* **442**, 38 (2007).

[22] S.W. Bruenn, *Astrophys. J. Suppl.* **58**, 771 (1985); A. Mezzacappa, S.W. Bruenn, *Astrophys. J.* **405**, 637 (1993); **410**, 740 (1993).

[23] A. Juodagalvis *et al.*, *Nucl. Phys.* **A747**, 87 (2005).

[24] K. Langanke, G. Martinez-Pinedo, P. von Neumann-Cosel, A. Richter, *Phys. Rev. Lett.* **93**, 202501 (2004).

[25] K. Langanke *et al.*, *Phys. Rev. Lett.* **100**, 011101 (2008).

[26] J. Pruet *et al.*, *Astrophys. J.* **623**, 1 (2005).

[27] C. Fröhlich *et al.*, *Astrophys. J.* **637**, 415 (2006).

[28] S. Wanajo, *Astrophys. J.* **647**, 1323 (2006).

[29] C. Fröhlich *et al.*, *Phys. Rev. Lett.* **96**, 142502 (2006).

[30] A. Frebel *et al.*, *Nature (London)* **434**, 871 (2005).

[31] J. Pruet, R. Hoffman, S.E. Woosley, H.T. Janka, *Astrophys. J.* **644**, 1028 (2006).

[32] E.M. Burbidge, G.R. Burbidge, W.A. Fowler, F. Hoyle, *Rev. Mod. Phys.* **29**, 547 (1957).

[33] A.G.W. Cameron, Chalk River Report CRL-41, 1957.

[34] J.J. Cowan, F.-K. Thielemann, J.W. Truran, *Phys. Rep.* **208**, 267 (1991).

[35] K.L. Kratz *et al.*, *Astrophys. J.* **402**, 216 (1993).

[36] S.E. Woosley *et al.*, *Astrophys. J.* **399**, 229 (1994).

[37] C. Freiburghaus, S. Rosswog, F.-K. Thielemann, *Astrophys. J.* **525**, L121 (1999).

[38] G.J. Wasserburg, M. Busso, R. Gallino, K.M. Nollett, *Nucl. Phys.* **A777**, 5 (2006).
[39] C. Sneden *et al.*, *Astrophys. J.* **591**, 936 (2003).
[40] P. Möller, J.R. Nix, K.L. Kratz, *At. Data Nucl. Data Tables* **66**, 131 (1997).
[41] I.N. Borsov, S. Goriely, J.M. Pearson, *Nucl. Phys.* **A621**, 307c (1997).
[42] M. Samyn, S. Goriely, J.M. Pearson, *Nucl. Phys.* **A725**, 69 (2003).
[43] S. Goriely, M. Samyn, J.M. Pearson, M. Onsi, *Nucl. Phys.* **A750**, 425 (2005).
[44] J.R. Stone, *J. Phys. G* **31**, 211 (2005).
[45] K.L. Kratz *et al.*, *J. Phys. G* **24**, S331 (1988).
[46] K.L. Kratz *et al.*, *Z. Phys.* **A325**, 489 (1986).
[47] J. Lettry *et al.*, *Rev. Sci. Instrum.* **69**, 761 (1998).
[48] T. Kurtukian-Nieto *et al.*, submitted to *Phys. Rev. Lett.*
[49] I.N. Borzov, *Phys. Rev.* **C67**, 025802 (2003).
[50] P. Moeller, B. Pfeiffer, K.-L. Kratz, *Phys. Rev.* **C67**, 055802 (2003).
[51] J. Engel *et al.*, *Phys. Rev.* **C60**, 014302 (1999).
[52] I.N. Borzov *et al.*, *Z. Phys.* **A355**, 117 (1996).
[53] I.N. Borzov *et al.*, submitted to *Nucl. Phys.* **A**.
[54] G. Martinez-Pinedo, K. Langanke, *Phys. Rev. Lett.* **83**, 4502 (1999).
[55] G. Martinez-Pinedo, *Nucl. Phys.* **A688**, 57c (2001).
[56] J.J. Cuenca-Garcia *et al.*, *Eur. J. Phys.* **A34**, 99 (2007).
[57] G.M. Fuller, B.S. Meyer, *Astrophys. J.* 453, 792 (1995).
[58] Y.-Z. Qian, W.C. Haxton, K. Langanke, P. Vogel, *Phys. Rev.* **C55**, 1532 (1997).
[59] W.C. Haxton, K. Langanke, Y.-Z. Qian, P. Vogel, *Phys. Rev. Lett.* **78**, 2694 (1997).
[60] Y.-Z. Qian, *Astrophys. J.* **569**, L103 (2002).
[61] E. Kolbe, K. Langanke, G.M. Fuller, *Phys. Rev. Lett.* **92**, 111101 (2004).
[62] A. Kelic *et al.*, *Phys. Lett.* **B616**, 48 (2006).
[63] J. Benlliure *et al.*, *Nucl. Phys.* **A628**, 458 (1998).
[64] G. Martinez-Pinedo *et al.*, *Prog. Part. Nucl. Phys.* **59**, 199 (2007).
[65] G. Martinez-Pinedo *et al.*, to be published.